



# Quantum Image Edge Detection Algorithm

Suzhen Yuan<sup>1</sup> · Salvador E. Venegas-Andraca<sup>2</sup> · Yuchan Wang<sup>1</sup> ·  
Yuan Luo<sup>1</sup> · Xuefeng Mao<sup>1</sup>

Received: 30 October 2018 / Accepted: 23 May 2019 / Published online: 3 June 2019  
© Springer Science+Business Media, LLC, part of Springer Nature 2019

## Abstract

Quantum image processing has been developing rapidly in recent years. In this paper, the edge detection algorithm for quantum images is proposed. Three steps are consisted: quantum image smoothing, finding the highlight gradient and quantum edge tracking. In order to implement the above processes, a quantum comparator is designed and quantum circuits for all the steps are given. The proposed quantum edge detection algorithm makes full use of quantum parallelism.

**Keywords** Quantum image processing · Edge detection · Quantum comparator

## 1 Introduction

Quantum computation and quantum information is a new interdisciplinary research field, involves physics, computer science, mathematics and information science [1]. It has been proved that quantum computation has great advantages in information theory, cryptography and image processing because of its parallel processing characteristics [2, 3]. Parallel processing means we can get all the values of function  $f(x)$  of different  $x$  values by just one calculation [4]. In recent years, there have been a lot of researches on quantum image processing, including the representation of an image in a quantum computer, such as Qubit Lattice model [5, 6], A flexible representations of quantum images (FRQI) [7], the multidimensional color image storage model [8], and the audio signals representation [9]. The previous image representation models use a single qubit to store the color information which represents the actual value of a physical parameter, but the intensity information is not stored on them. Thus, many complexity operations involving intensity information cannot be done based on these representation models. To improve this drawback, the novel enhanced quantum representation

---

✉ Suzhen Yuan  
yusuzh2012@126.com

✉ Yuchan Wang  
wangyuchan@cqupt.edu.cn

<sup>1</sup> College of opto electronic engineering, Chongqing University of Posts and Telecommunications, Chongqing 400065, China

<sup>2</sup> Tecnológico de Monterrey – Escuela de Ciencias e Ingeniería, 52926 Estado de México, Mexico

(NEQR) model [10] is proposed. NEQR uses a normalized superposition of  $(2n + q)$  qubits to store an image, where the  $2n$  qubits represent position information and the  $q$  qubits represent grayscale intensity information. Therefore, if image intensity is a key parameter to be controlled, the NEQR model is a suitable choice. For a concise review of quantum image representations, we kindly refer the reader to [11].

By exploiting these representation models, various operations are designed by applying standard quantum operators such as the NOT gate and Hadamard gates, combined with appropriate quantum measurement operators [12]. For example, infrared images processing algorithms are presented based on the improved Qubit Lattice model [13]. In addition, geometric transformations [14] and color transformations [15] are proposed based on the FRQI representation. Moreover, some applications, such as a strategy for watermarking and authentication quantum images [16, 17], a framework for producing movies on quantum computers [18], segmentation algorithms [19], quantum image matching [20], and security technologies [21] have been proposed based on these representation models.

Image is an important source for human beings to acquire and exchange information. Therefore, image processing involves many aspects of human life, including aviation, aerospace, biomedical engineering, communication engineering and robot vision [22]. Images carry so much information which comes with large data size. To process image, we have to abstract important information from the large amount of data. Image edge detection can eliminate the irrelevant information of an image and extract the meaningful features, thus reduce the amount of information. It is also the basis of further works, such as pattern recognition, analysis and understanding. In this paper, we propose a quantum version of edge detector framework based on the NEQR model. The quantum edge algorithm consists of three main steps, including the image smoothing, finding the highlight gradient and the edge tracking. The quantum comparator is designed to compare the value of a pixel with its neighborhoods, which can be used to perform the gradient direction, non-maximum suppression and hysteresis thresholding.

The rest of this paper is organized as follows. In Sect 2, the NEQR representation model is provided. The quantum edge detection algorithm is proposed in Sect 3. Section 4 gives the discussion and Sect 5 draws the conclusion.

## 2 NEQR Representation Model

A classical gray image is stored as a matrix. One element of the matrix represents the gray-scale information of a pixel in the same position of the image, and the whole image has to be processed one pixel by one pixel [22]. The NEQR model is proposed in [10]. Suppose that the gray range of a  $2^n \times 2^n$  quantum image is  $2^q$ , binary sequence  $G_{YX}^0 G_{YX}^1 \cdots G_{YX}^{q-2} G_{YX}^{q-1}$  encodes the gray-scale value  $f(Y, X)$  of the corresponding pixel  $(Y, X)$  as in (1).

$$f(Y, X) = G_{YX}^0 G_{YX}^1 \cdots G_{YX}^{q-2} G_{YX}^{q-1}, G_{YX}^k \in [0, 1], f(Y, X) \in [0, 2^q - 1] \quad (1)$$

where  $Y, X$  are two  $n$ -bit binary sequences that store the position information of a pixel. These  $2n + q$  qubits store the whole image which can be written as in (2),

$$|I\rangle = \frac{1}{2^n} \sum_{Y=0}^{2^n-1} \sum_{X=0}^{2^n-1} |f(Y, X)\rangle |YX\rangle = \frac{1}{2^n} \sum_{Y=0}^{2^n-1} \sum_{X=0}^{2^n-1} \bigotimes_{i=0}^{q-1} |G_{YX}^i\rangle |YX\rangle \quad (2)$$

There are two parts in the NEQR representation of an image.  $\bigotimes_{i=0}^{q-1} |G_{YX}^i\rangle$  and  $|YX\rangle$  encode the grayscale information and their corresponding positions of the image, respectively. For the 2-D image, the position information  $|YX\rangle$  includes two parts: the vertical and the horizontal coordinates. For  $2n \times 2n$  image, the vector  $|YX\rangle$  can be written as

$$|YX\rangle = |y_{n-1}, y_{n-2}, \dots, y_0\rangle |x_{n-1}, x_{n-2}, \dots, x_0\rangle, x_i, y_i \in \{0, 1\} \quad (3)$$

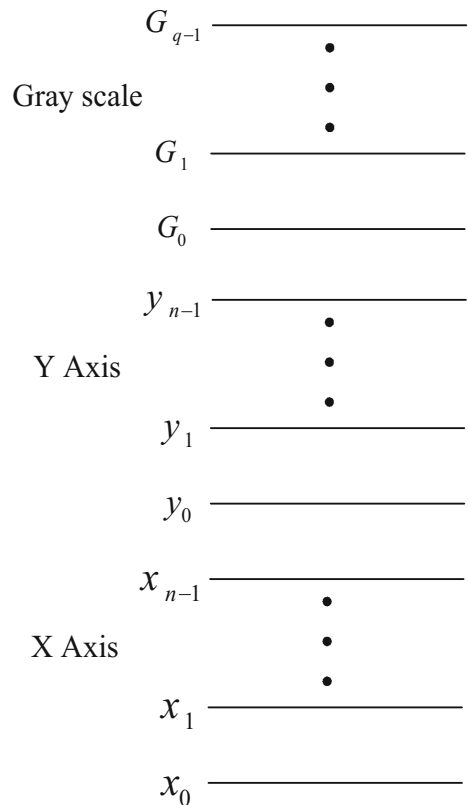
The first  $n$ -qubit  $y_{n-1}, y_{n-2}, \dots, y_0$  encodes the vertical location information and the second  $n$ -qubit  $x_{n-1}, x_{n-2}, \dots, x_0$  encodes the horizontal location information. The quantum circuit structure of NEQR is shown in Fig. 1.

Figure 2 shows a  $4 \times 4$  NEQR image example in which  $f(Y, X)$  denotes the grayscale value of pixel  $(Y, X)$ .

Figure 3 is a  $2 \times 2$  grayscale image ranges between 0 and 255. In this example, 2 qubits are needed to store the position information and 8 qubits are needed to store the grayscale information. Thus, the NEQR model for this image can be written as

$$|I\rangle = \frac{1}{2} \left( |255\rangle|00\rangle + |192\rangle|01\rangle + |127\rangle|10\rangle + |0\rangle|11\rangle \right) \\ = \frac{1}{2} \left( |11111111\rangle|00\rangle + |11000000\rangle|01\rangle + |01111111\rangle|10\rangle + |00000000\rangle|11\rangle \right) \quad (4)$$

**Fig. 1** The quantum circuit of NEQR model



**Fig. 2** A  $4 \times 4$  image represented by the NEQR model.  $f(Y, X)$  denotes the grayscale value of pixel  $(Y, X)$

		$X$			
		<div> <div>00</div> <div>01</div> <div>10</div> <div>11</div> </div>			
$Y$	00	$f(00,00)$	$f(00,01)$	$f(00,10)$	$f(00,11)$
	01	$f(01,00)$	$f(01,01)$	$f(01,10)$	$f(01,11)$
	10	$f(10,00)$	$f(10,01)$	$f(10,10)$	$f(10,11)$
	11	$f(11,00)$	$f(11,01)$	$f(11,10)$	$f(11,11)$

Every item of the superposition state represents a pixel of the image, and an image can be processed just by one calculation because of the superposition state. This means when a pixel is operated, then all the pixels of the image are operated, which is called the parallel processing characteristics of quantum computing.

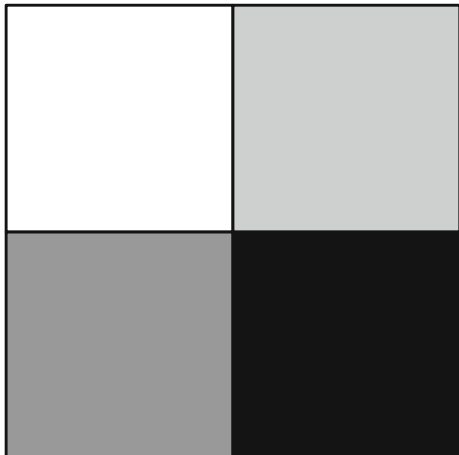
### 3 The Quantum Edge Detection Algorithm

The quantum edge detection algorithm consists of three main steps: image smoothing, finding the highlight gradient and edge tracking.

#### 3.1 Quantum Image Smoothing

The derivative is very sensitive to noise, so a Gauss smoothing filter is needed to blur the original image and reduce noise. The size and standard deviation  $\sigma$  of the Gauss filter differs in different conditions in order to find the optimal edge. The smoothing can be obtained by calculating the convolution between the Gaussian mask and the image.

**Fig. 3** A  $2 \times 2$  image, the gray value of the four pixels are 255, 192, 127 and 0



Quantum convolution is happened between an image and a mask. The convolution process needs multiplying the corresponding coefficient of the mask with the gray information of the quantum image, then adding up the results to obtain the response. Since the quantum convolution is already designed in reference [23]. They can be directly used in this paper. An example can be given to explain the whole process of quantum convolution. Suppose that the size of the mask is  $3 \times 3$ , i.e.  $k = 1$ , and the mask is given by Eq. (5).

$$\begin{bmatrix} 0 & -1 & 0 \\ -1 & 4 & -1 \\ 0 & -1 & 0 \end{bmatrix} \quad (5)$$

Then, the quantum image set in Eq. (9) of reference [23] would be

$$\left\{ |I_{Y-1,X}\rangle, |I_{Y,X-1}\rangle, |I_{Y,X}^{Y,X}\rangle, |I_{Y,X+1}\rangle, |I_{Y+1,X}\rangle \right\} \quad (6)$$

The convolution process is realized by the following calculation

$$|\varphi_1\rangle = U_{Mu} \left\{ 4 \right\} |I_{YX}\rangle \quad (7)$$

$$|\varphi_2\rangle = QADD \left( |I_{Y-1,X}\rangle, |I_{Y,X-1}\rangle, |I_{Y,X+1}\rangle, |I_{Y+1,X}\rangle \right) \quad (8)$$

$$|\psi\rangle = QSUB \left( |\varphi_1\rangle, |\varphi_2\rangle \right) \quad (9)$$

Where  $U_{Mu}$  is the quantum multiplier operator as shown in Fig. 6 of reference [23],  $QADD$  is the quantum full adder as shown in Fig. 3 of reference [23], and  $|\psi\rangle$  is the convolution result.

In this smoothing step, we just need to change the mask in Eq. (5) to the Gaussian mask.

The time complexity of the convolution is determined by the position shifting operation and the quantum multiplier operation designed in [23]. The needed number of the position shifting operation and the quantum multiplier operation is proportional to the size of the mask, so the time complexity of the convolution is  $O(k^2n^2 + k^2q^3)$ .

### 3.2 Finding the Highlight Gradient

#### 3.2.1 Calculate the Gradient

The direction of the image edge may be different in different position, so four masks are used to calculate the gradient in four different discrete directions, horizontal, vertical,  $45^\circ$  and  $135^\circ$ . Figure 4

-1	0	1	1	2	1	0	1	2	2	1	0
-2	0	2	0	0	0	-1	0	1	1	0	-1
-1	0	1	-1	-2	-1	-2	-1	0	0	-1	-2
(a)			(b)			(c)			(d)		

**Fig. 4** Four masks. (a) The direction of gradient is horizontal. (b) The direction of gradient is vertical. (c) The direction of gradient is  $45^\circ$ . (d) The direction of gradient is  $135^\circ$

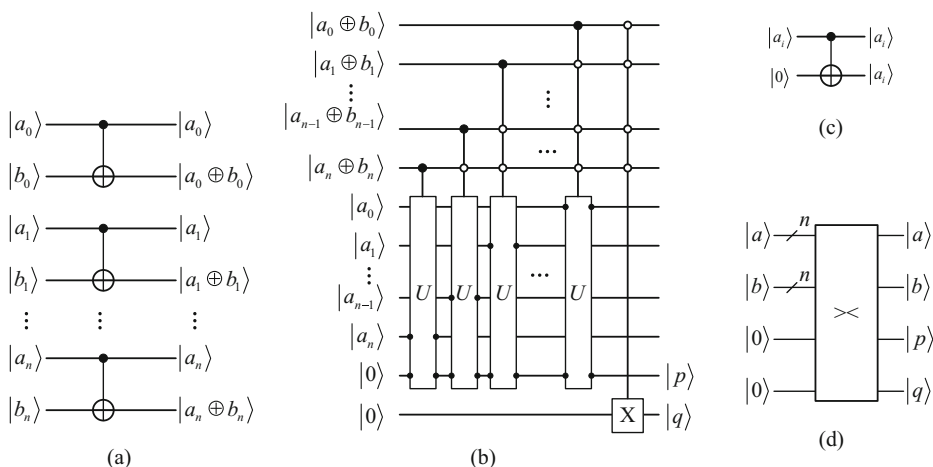


**Fig. 5** **a** XOR operation on two binary numbers. **b** Quantum comparator. **c** The detail quantum circuit of Quantum gate  $U$  in (b). **d** Simplified quantum comparator

shows one choice of the masks. These four gradients  $|g_0\rangle$ ,  $|g_{45}\rangle$ ,  $|g_{90}\rangle$  and  $|g_{135}\rangle$  can be obtained by calculating the convolution between the mask and the image. The maximum  $g_m(Y, X)$  of the four gradients will be the potential real gradient and its direction can be regarded as the edge direction in pixel  $(Y, X)$ . So a gradient image and its corresponding direction are gotten.

### 3.2.2 Quantum Comparator

To find the maximum of the four gradients, a quantum comparator is proposed, which can compare the value of two binary numbers. To compare the two binary numbers, we need to compare every bit of them. Assume that we get 1 when they are different and 0 when they are the

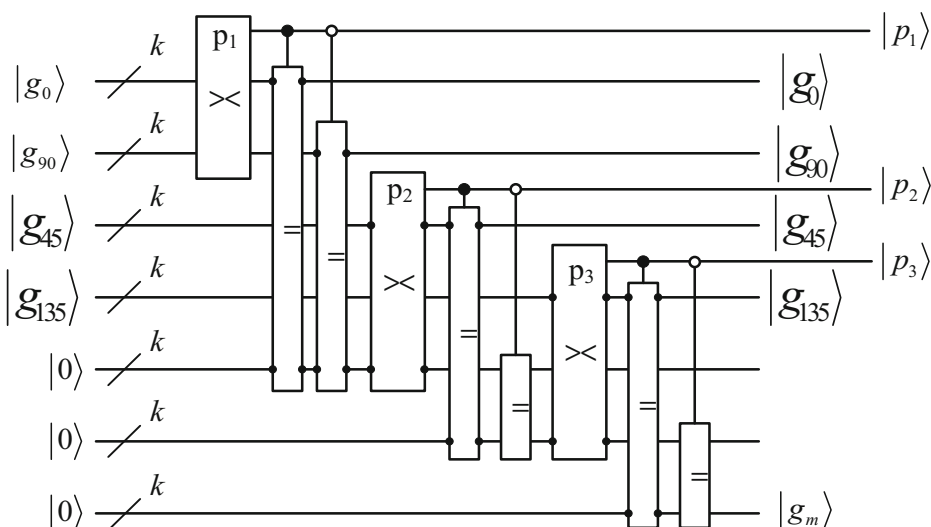


**Fig. 6** Quantum circuit of the gradient and its direction

**Table 1** Truth table of  $p_3p_2p_1$ 

$p_3p_2p_1$	000	001	010	011	100	101	110	111
Maximum	$g_{135}$	$g_{135}$	$g_{135}$	$g_{135}$	$g_{45}$	$g_{45}$	$g_{90}$	$g_0$
Direction	135	135	135	135	45	45	vertical	horizontal

same. For example, we get 00110 when compare 10,011 with 10,101. Then we just need to detect the first 1 of the sequence 00110 and compare the corresponding bit of 10,011 and 10,101.

Figure 5a shows the quantum circuit to compare every bit of the two binary numbers. Figure 5b shows the quantum circuit to detect the first different bit and get the result which is stored in  $|p\rangle$  and  $|q\rangle$ . Figure 5c shows the detail quantum circuit of the controlled quantum gate in Fig. 5b. Fig. 5d shows the simplified quantum comparator.

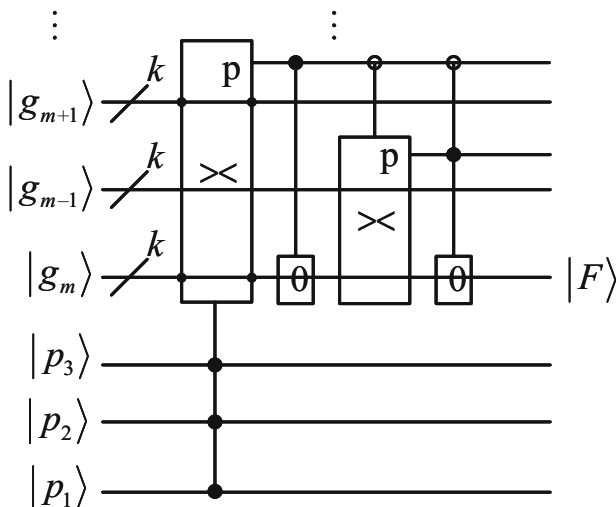
### 3.2.3 Find the Direction of the Gradient

Figure 6 shows the detail quantum circuit to find the gradient, where three quantum comparators are used to find the maximum of the four gradients and only  $|p\rangle$  is used in every quantum comparator. The quantum gate with an equal sign can copy  $k$  qubits to another  $k$  qubits with an initial state  $|0\rangle^{\otimes k}$ , which can be easily realized using  $k$  CNOT gates.

The maximum gradient  $|g_m\rangle$  will be the real gradient and the direction information is in  $|p_1p_2p_3\rangle$  as is shown in Table 1.

### 3.2.4 Non-maximum Suppression

In 3.2.3, we obtained the gradient image  $|g_m\rangle$  and the direction of the gradient. The gradient will be checked whether it is the maximum of its neighbors in the corresponding direction, if not, this pixel will have to be set to 0. For example, for a  $3 \times 3$  neighborhood and the direction of the gradient is horizontal, the condition in which the pixel will be set to 0 is that  $g_m(Y, X) < g_m(Y, X-1)$  or  $g_m(Y, X) < g_m(Y, X+1)$ .

**Fig. 7** Quantum circuit of non-maximum suppression

**Fig. 8** Utilize two CNOT gates to exchange two qubits

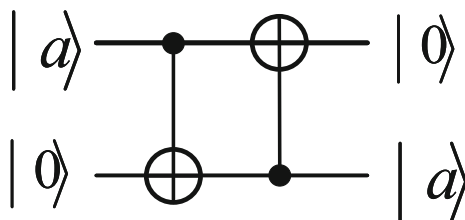


Figure 7 shows a quarter of the quantum circuit of the non-maximum suppression, which is the quantum circuit when the gradient direction is horizontal and controlled qubits  $p_3p_2p_1 = 111$ . When  $p_3p_2p_1$  equals to other numbers, the quantum circuit is similar, and the difference is that  $|g_{m+1}\rangle$  and  $|g_{m-1}\rangle$  must be two adjacent pixels of  $|g_m\rangle$  in certain direction corresponding to  $p_3p_2p_1$ . The quantum gate with a 0 can set these  $k$  qubits to 0, which can be done using the quantum circuit shown in Fig. 8  $k$  times.  $|F\rangle$  is the output. Figure 8 can transform the quantum state  $|a, 0\rangle$  into  $|0, a\rangle$ , which means the two qubits  $|a\rangle$  and  $|0\rangle$  are exchanged.

### 3.3 Edge Tracking

#### 3.3.1 Hysteresis Thresholding

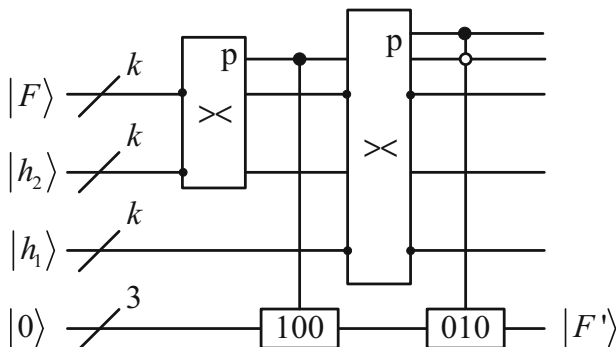
In order to find the actual edge, two threshold  $h_1$  and  $h_2$  are used. Here  $h_1 < h_2$  and  $h_1, h_2$  are selectable in different condition. If  $g_m > h_2$ , the pixel will be judged strong edge; if  $h_1 < g_m < h_2$ , the pixel will be judged weak edge; if  $g_m < h_1$ , the pixel will be set to 0.

Figure 9 shows the quantum circuit of edge tracking. The quantum gate with certain number on can set  $|0\rangle^{\otimes 3}$  to certain value, which can be done with some NOT gates on certain qubits.

After the hysteresis thresholding, there are only three types of pixels with different values, which are shown in Table 2.

#### 3.3.2 Edge Linking

The purpose of this step is to link the edges as a line with single pixel. Every weak edge pixel will be checked if there is at least a strong edge pixel in the neighborhood; if so, the pixel will be judged a new strong edge, otherwise the pixel will be set to 0. Now the pixel is either a



**Fig. 9** Quantum circuit of hysteresis thresholding



**Table 2** Three types of pixels with three values

Value	Type
100	Strong edge pixel
010	Weak edge pixel
000	Non-edge pixel

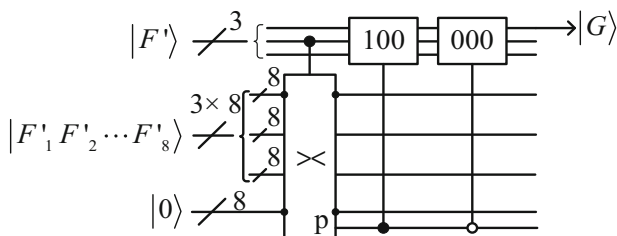
strong edge pixel or 0, and a binary edge image is get. The detailed steps to realize the quantum edge detection algorithm are described in the following subsection.

For a  $3 \times 3$  neighborhood, the adjacent pixels of  $|F'\rangle$  can be prepared using the way introduced in part 2 of reference [23]. Figure 10 shows the detail quantum circuit to link the edge. Every bit of  $|F'_1 F'_2 \cdots F'_8\rangle$  composes a new 8-bit sequence, we compare the top one with  $|00000000\rangle$  to check whether there is at least one strong edge pixel around  $|F'\rangle$ . In the end, all the weak edge pixels are either converted to strong edge pixels or set to 0; we get a binary edge image on the bit  $|G\rangle$ , which is the top bit of  $|F'\rangle$ .

## 4 Discussion

The last step of image processing is usually the image retrieve. Quantum measurement is a unique way to recover classical information from a quantum state. Considering the objectives pursued by quantum image edge detection, the edge detection may be used as a pre-processing step of other quantum image processing algorithms such as image segmentation and object recognition, or as the final step of a computational process. In the first situation, the edge detection is an intermediate step, which could simply be passed to the next quantum algorithms, hence making quantum measurement an unnecessary step. In the second situation, the result of the filtering is the last part of a quantum routine, information retrieval could be done. Subsection 4.1 of reference [9] gives the detailed retrieval scheme.

The algorithm proposed in this paper has great superiority and the parallelism of quantum computation is fully utilized. The NEQR representation model adopts a quantum superposition state to represent an image. When one quantum gate operates on a pixel, it will operate on all the pixels at the same time, which makes the algorithm have low time complexity. For example, suppose a  $2^n \times 2^n$  image and a  $k \times k$  template, the needed simple operations are  $O(k^2 \times 2^{2n})$  in a classical computer for the convolution operation, but it is  $O(k^2 n^2 + k^2 q^3)$  in the quantum version. The convolution is a very important operation in this algorithm. It is obvious that the quantum algorithm has great advantages.

**Fig. 10** Quantum circuit of edge linking

## 5 Conclusion

In this paper we developed a quantum version for edge detection algorithm which makes full use of quantum parallelism. This is an important pre-processing operation in many image processing algorithms. It is usually applied in the early stages of computer vision. A quantum comparator is designed to actualize the quantum edge detection algorithm. Three steps, image smoothing, finding the highlight gradient and edge tracking, are included. We also design the corresponding quantum circuits of these steps.

The quantum image processing field is still in its infant. The result obtained in this paper could be used in more quantum image processing algorithms. In the future, we will working at the development of new quantum image processing algorithm base on the quantum image edge detection.

**Acknowledgments** This work is supported by the National Natural Science Foundation of China (Grant No: 61801061), the Natural Science Foundation of Chongqing City (Grant No: CSTC2016jcyjA0028, CSTC2017jcyjA0893, CSTC2017jcyjAX0427), the Scientific and Technological Research Program of Chongqing Municipal Education Commission (Grant No: KJQN201800607, KJ1704090).

## References

1. Feynman, R.: Simulating physics with computers. *Int. J. Theor. Phys.* **21**, 467–488 (1982)
2. Shor, P.W.: Algorithms for quantum computation: discrete logarithms and factoring. In: *Proceedings of 35th Annual Symposium on Foundations of Computer Science*. Los Almitos, pp. 124–134, USA (1994)
3. Grover, L.: A fast quantum mechanical algorithm for database search. In: *Proceedings of the 28th Annual Symposium on the Theory of Computing*, pp. 212–219, Philadelphia, USA (1996)
4. Nielsen, M.A., Chuang, I.L.: *Quantum Computation and Quantum Information*. Cambridge. Cambridge Univ Press (2000)
5. Venegas-Andraca, S.E., Bose, S.: Storing, processing and retrieving an image using quantum mechanics. *Stochastic Environmental Research & Risk Assessment*. **5105**, 1085–1090 (2003)
6. Venegas-Andraca, S.E., Bose, S.: Quantum computation and image processing: new trends in artificial intelligence. In: *Proceedings of the International Conference on Artificial Conference on Artificial Intelligence IJCAI-03*, Mexico, pp. 1563–1564 (2003)
7. Le, P.Q., Dong, F., Hirota, K.: A flexible representation of quantum images for polynomial preparation, image compression and processing operations. *Quantum Inf. Process.* **10**, 63–84 (2011)
8. Li, H., Zhu, Q., Zhou, R., Lan, H.: Multidimensional color image storage, retrieval, and compression based on quantum amplitudes and phases. *Inf. Sci.* **273**(3), 212–232 (2014)
9. Yan, F., Iliyasu, A.M., Guo, Y., Yang, H.: Flexible representation and manipulation of audio signals on quantum computers. *Theor. Comput. Sci.* **752**, 71–85 (2018)
10. Zhang, Y., Lu, K., Gao, Y., Wang, M.: NEQR: a novel enhanced quantum representation of digital images. *Quantum Inf. Process.* **12**, 2833–2860 (2013)
11. Yan, F., Iliyasu, A.M., Venegas-Andraca, S.E.: A survey of quantum image representations. *Quantum Inf. Process.* **15**(1), 1–35 (2016)
12. Childs, A.M., Leung, D.W., Nielsen, M.A.: Unified derivations of measurement-based schemes for quantum computation. *Phys. Rev. A*. **71**(3), 309–315 (2004)
13. Yuan, S., Mao, X., Xue, Y., Chen, L., Xiong, Q., Compare, A.: SQR: a simple quantum representation of infrared images. *Quantum Inf. Process.* **13**, 1353–1379 (2014)
14. Le, P.Q., Iliyasu, A.M., Dong, F., et al.: Fast geometric transformations on quantum images. *IAENG International Journal Applied Mathematics*. **40**, 113–123 (2010)
15. Le, P.Q., Iliyasu, A.M., Dong, F., et al.: Efficient Color Transformations on Quantum Images. *JACIII*, vol. 15, pp. 698–706 (2011)
16. Iliyasu, A.M., Le, P.Q., Dong, F., et al.: Watermarking and authentication of quantum images based on restricted geometric transformations. *Info. Sci.* **186**, 126–149 (2011)

17. Iliyasu, A.M., Le, P.Q., Yan, F., et al.: A two-tier scheme for greyscale quantum image watermarking and recovery. *Int. J. Innov. Comput. Appl.* **5**(2), 85–101 (2013)
18. Iliyasu, A.M., Le, P.Q., Dong, F., et al.: A framework for representing and producing movies on quantum computers. *Intl. J. of Quantum Info.* **9**, 1459–1407 (2011)
19. Caraiman, S., Manta, V.I.: Image segmentation on a quantum computer. *Quantum Inf. Process.* **14**(5), 1693–1715 (2015)
20. Jiang, N., Dang, Y., Wang, J.: Quantum image matching. *Quantum Inf. Process.* **15**(9), 3543–3572 (2016)
21. Yan, F., Iliyasu, A.M., Le, P.Q.: Quantum image processing: a review of advances in its security technologies[J]. *International Journal of Quantum Information.* **15**(3), 1730001 (2017)
22. Rafael, C.G., Richard, E.W., Steven, L.E.: *Digital Image Processing*, 4th edn. House of Electronics Industry Press, Beijing (2002)
23. Yuan, S., Lu, Y., Mao, X., Luo, Y., Yuan, J.: Improved quantum image filtering in the spatial domain. *Int. J. Theor. Phys.* **57**(3), 804–813 (2018)

**Publisher's Note** Springer Nature remains neutral with regard to jurisdictional claims in published maps and institutional affiliations.